

Beacon: A Naturalistic Driving Dataset During Blackouts for Benchmarking Traffic Reconstruction and Control

Supriya Sarker¹, Iftekharul Islam¹, Bibek Poudel¹, and Weizi Li¹

Abstract—Extreme weather events and other vulnerabilities are causing blackouts with increasing frequency, disrupting traffic control systems and posing significant challenges to urban mobility. To address this growing concern, we introduce Beacon, a naturalistic driving dataset collected during blackouts at complex intersections. Beacon provides detailed traffic data from two unsignalized intersections in Memphis, TN, including timesteps, origin, and destination lanes for each vehicle over four hours. We analyze traffic demand, vehicle trajectories, and density across different scenarios. We also use the dataset to reconstruct unsignalized, signalized and mixed traffic conditions, demonstrating its utility for benchmarking traffic reconstruction techniques and control methods. To the best of our knowledge, Beacon could be the first public available traffic dataset that captures naturalistic driving behaviors at complex intersections.

I. INTRODUCTION

Modern urban infrastructure, especially in densely populated areas, is increasingly vulnerable to disruptions caused by extreme weather events and other factors. These disturbances often lead to significant power outages, incapacitating critical urban systems, with traffic control mechanisms being notably affected [1]. Traffic lights, the backbone of urban traffic management, rely entirely on electricity. Thus, their failure during blackouts leads to increased congestion and accident risks, especially at intersections. These critical nodes, crucial for multi-directional traffic flow, are also hotspots for over 45% of U.S. traffic crashes [2]. During blackouts, intersections can remain without control for extended periods and cause widespread gridlock to a city [3], [4].

To address these challenges and develop effective traffic management solutions for blackout scenarios, comprehensive datasets representing real-world traffic behavior during power outages are essential. However, capturing such a dataset is rare, as orchestrating a controlled blackout for data collection is impractical and potentially unsafe, making naturally occurring events the only feasible, though infrequent, opportunities for gathering this type of data.

In response to this critical need, we introduce Beacon, a dataset containing four hours of traffic dynamics during peak periods including midday and afternoon, captured during a blackout in Memphis, TN, USA. Beacon provides detailed traffic movements at two real-world intersections (Fig. 1), offering information such as timing, origin, and destination lanes for each vehicle navigation the intersections. This naturalistic driving dataset presents a unique opportunity

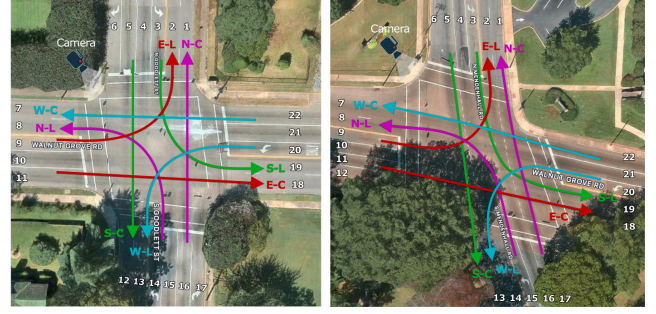


Fig. 1. Satellite views of the studied intersections with lane numbering and traffic flow directions.

to study and analyze traffic behavior under unsignalized conditions.

Using the dataset, we simulate three different types of traffic control - (i) unsignalized traffic control, (ii) signalized traffic control, and (iii) mixed traffic control as a showcase of the usage of the dataset. We conduct a thorough analysis of unsignalized intersections using Beacon. We outline the processes of data collection, extraction, and reconstruction, and provide in-depth examination of the traffic dynamics at these intersections. Through this detailed analysis and reconstruction, we aim to contribute insights to the development of more resilient urban traffic systems that function during power disruption.

II. RELATED WORK

A. Traffic Reconstruction and Control

Sanchez *et al.* uses the Caltrans Performance Measurement System (PeMS) dataset, which provides sparse traffic data from sensors across California highways [5]. To overcome data limitations, the authors propose a kernel-based traffic reconstruction method, simulating detailed vehicle trajectories to create a continuous, spatio-temporal traffic dataset. This method identifies SAG events by applying a kernel designed to detect speed oscillations and uses bootstrapping to quantify uncertainty, generating multiple traffic scenarios for robust detection. The approach enables precise identification of congestion "hotspots," offering insights to policymakers for targeted congestion interventions.

Wang *et al.* proposes a novel method called Temporal and Adaptive Spatial Constrained Low Rank (TAS-LR) for reconstructing missing traffic data [6]. This method uses low-rank matrix factorization to analyze both spatial and temporal correlations within traffic data. Implementation involves

¹Supriya Sarker, Iftekharul Islam, Bibek Poudel, and Weizi Li are with Min H. Kao Department of Electrical Engineering and Computer Science at University of Tennessee, Knoxville, TN, USA {mislam73, ssarker8, bpoudel13}@vols.utk.edu; weizili@utk.edu

decomposing the traffic matrix into two factor matrices, representing spatial features (road link characteristics) and temporal features (traffic patterns). The model leverages six real-world datasets, which include data from road links, speed, and volume metrics, making it adaptable to various traffic scenarios.

Kataoka *et al.* proposes a method for reconstructing missing traffic data using Markov Random Field (MRF) modeling [7]. The process involves using a Bayesian approach with MRFs to model the spatial dependencies in traffic data, estimating unobserved data by solving a system of equations via a mean-field method. The datasets include simulated road network data from Sendai, Japan, which reflects real traffic patterns.

Bilotta and Nesi propose a traffic flow reconstruction model that addresses the indeterminacy in traffic distribution at junctions using a stochastic relaxation technique [8]. The method involves solving a partial differential equation (PDE) for traffic flow and estimating traffic distribution at junctions by computing a Traffic Distribution Matrix (TDM) based on real-time sensor data.

Qi *et al.* proposes a method for reconstructing vehicle trajectories on urban road networks using Automatic License Plate Recognition (ALPR) data [9]. The implementation involves dividing vehicle trips based on travel time, generating candidate paths through an improved K-shortest-path (P-KSP) algorithm, and selecting the optimal trajectory using an auto-encoder model. The dataset comprises ALPR data from an urban network in Ningbo, China, with vehicle detection information.

Feng *et al.* proposes a vehicle trajectory reconstruction method using Automatic Vehicle Identification (AVI) and traffic count data within a particle filter framework [10]. The process combines spatial-temporal trajectory correction factors, such as path consistency, AVI measurability, travel time consistency, gravity flow model, and path-link flow matching, to estimate vehicle paths accurately. Implementation is tested on a simulated urban network in Beijing using VISSIM, with results showing high accuracy in both trajectory reconstruction and OD matrix estimation when AVI coverage is at least 50%.

Bellini *et al.* proposes a traffic flow reconstruction method for urban areas using data from a limited number of fixed sensors [11]. The method models traffic dynamics with differential equations and fluid dynamics on a city graph, estimating road segment capacities using stochastic learning. Implementation involves loading city graph data, updating sensor values, assigning weights to road segments, and iteratively calculating traffic density, which is then visually represented on a map. Using traffic sensor data from Florence, Italy, the model achieves around 75% accuracy, making it significant for real-time urban traffic monitoring.

Bakowski and Radziszewski analyze changes in urban traffic parameters and noise levels before and after road reconstruction on a national road segment in Kielce, Poland [12]. The study utilized traffic flow and noise data collected between 2011 and 2016, applying statistical and bootstrap methods to account for data gaps. Results showed that road

reconstruction led to a decrease in noise levels despite a subsequent traffic increase. Using their proposed method the authors validated the Cnossos-EU noise model, aiding in assessing environmental impacts of urban roadworks.

Čičić *et al.* proposes a method for reconstructing traffic states and controlling congestion using Connected Automated Vehicles (CAVs) as mobile sensors and actuators [13]. The approach employs a model that simulates traffic flow using CAVs to measure local traffic density and act as controlled moving bottlenecks to dissipate stop-and-go waves. Simulated freeway data, based on the Cell Transmission Model (CTM), demonstrates how subsets of CAVs can efficiently estimate traffic density and reduce congestion delay.

B. Datasets for Traffic Reconstruction in Simulators

Another significance of traffic datasets is to facilitate simulators to deploy and validate to generate and analyze particular traffic scenarios. For mapping integration of AI and safety applications in traffic accident reconstruction, Shen *et al.* conducts a scientometric analysis on traffic collision scene reconstruction research from 2001 to 2021 using software tools like CiteSpace, VOSviewer, and SciMAT [14]. Li *et al.* introduces ScenarioNet, an open-source platform for large-scale traffic scenario simulation and modeling aimed at enhancing autonomous driving (AD) research [15]. The proposed method collects traffic data from multiple real-world sources, including the Waymo [16], nuScenes [17], and Argoverse [18] datasets, and standardizes it into a unified scenario description format. This data is then simulated in the MetaDrive [19] simulator, which supports tasks such as single-agent and multi-agent learning, AD stack testing, and scenario generation. By consolidating diverse traffic scenarios, ScenarioNet provides a comprehensive benchmark for AD safety evaluation, addressing challenges of data integration and cross-dataset scenario generation. The platform significantly improves AD system training by offering varied, realistic simulations for more robust and generalized learning.

III. DATA COLLECTION AND ANALYSIS

A. Location and Time

Our study focuses on traffic control during a blackout period in Memphis, TN, USA. Fig. 1 presents satellite views of the two intersections where video data was collected: Walnut Grove-Goodlett Street (latitude: 35.131508, longitude: -89.925530) (left) and Walnut Grove-Mendenhall Road (latitude: 35.130825, longitude: -89.898503) (right). We use intuitive acronyms: GWG-N and GWG-AN for the scenarios in the Walnut Grove-Goodlett Street at noon (12:00 PM-1:00 PM) and afternoon (5:00 PM-6:00 PM), respectively. For Walnut Grove-Mendenhall Road scenario at noon (12:27 PM-1:27 PM) and afternoon (5:21 PM-6:21 PM), we use WGM-N and WGM-AN, respectively. The data collection was conducted on a weekday, capturing both midday and afternoon peak periods to provide a comprehensive view of traffic patterns under these circumstances.

B. Data Annotation Process

The quality of the dataset heavily depends on the quality of data labeling. Beacon dataset is annotated by a human annotator from collected traffic videos and later validated by two other human annotators. The age group of these human annotators ranges from 25 to 35 years.

C. Data Analysis

This subsection presents a comprehensive analysis of the traffic demand, vehicle trajectories, and traffic density across the four scenarios.

1) *Traffic Demand Analysis*: Table I presents the traffic demand for each scenario, broken down by direction. The data reveals significant variations in traffic volume and directional flow across different times and locations. The Walnut Grove-Goodlett intersection experiences the highest total demand during the afternoon peak (5:00-6:00 PM) with 2,453 vehicles. Conversely, the same intersection sees the lowest demand during midday (12:00-1:00 PM) with 1,983 vehicles.

TABLE I
TRAFFIC DEMAND TABLE

Intersection Scene	North-bound	South-bound	East-bound	West-bound	Total Demand
GWG-N	280	410	685	608	1983
GWG-AN	425	629	794	605	2453
WGM-N	403	434	527	669	2033
WGM-AN	494	523	625	700	2342

Interestingly, directional patterns differ between the two intersections. At Walnut Grove-Goodlett intersection (Scenarios GWG-N and GWG-AN), eastbound traffic consistently dominates, while at Walnut Grove-Mendenhall intersection (Scenarios WGM-N and WGM-AN), westbound traffic is predominant.

2) *Vehicle Trajectory Analysis*: Figure 2, 3, 4 and 5 present transition of vehicles from start lanes to end lanes for each scenario, providing deeper insights into the traffic flow patterns.

Both intersections demonstrate strong east-west traffic flows along Walnut Grove Road, indicating its role as a major arterial route. At Walnut Grove-Goodlett intersection, the most significant movements during the afternoon peak are westbound (248 vehicles) and eastbound (228 vehicles) through movements. Walnut Grove-Mendenhall intersection exhibits more balanced east-west flows, with consistent high volumes in both directions throughout the day.

Turning behaviors at these intersections during the blackout reveal interesting patterns that vary by direction and location. At Walnut Grove-Goodlett intersection, we notice a strong preference for northbound right turns over left turns in both scenarios, while southbound left turns outnumber right turns. The pattern differs at Walnut Grove-Mendenhall intersection, where northbound left turns significantly surpasses right turns in both scenarios. These differences in turning preferences are likely linked to the surrounding road network, and the destinations accessible from each turn.

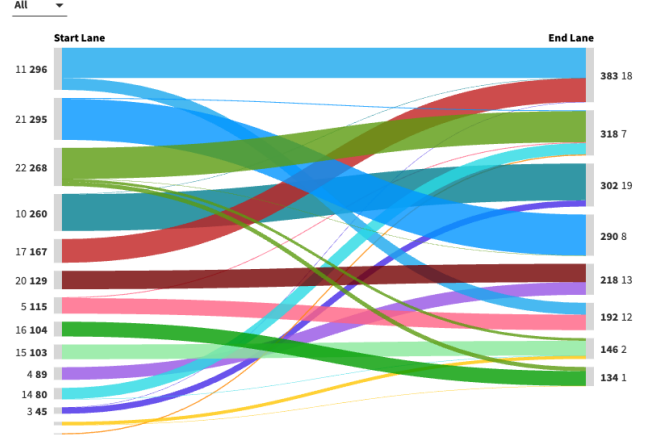


Fig. 2. Transition from start lane to end lane in scenario GWG_N

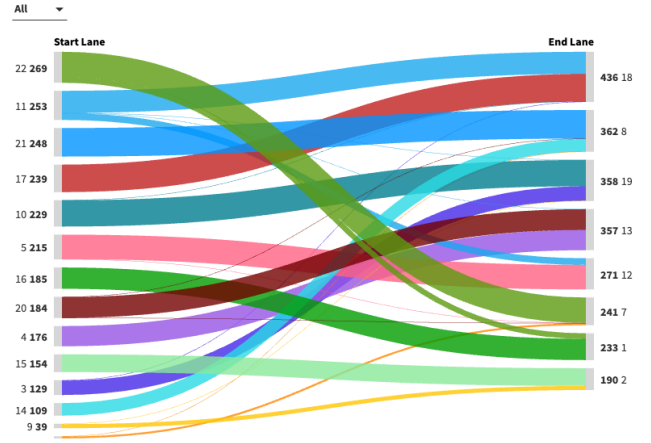


Fig. 3. Transition from start lane to end lane in scenario GWG_AN

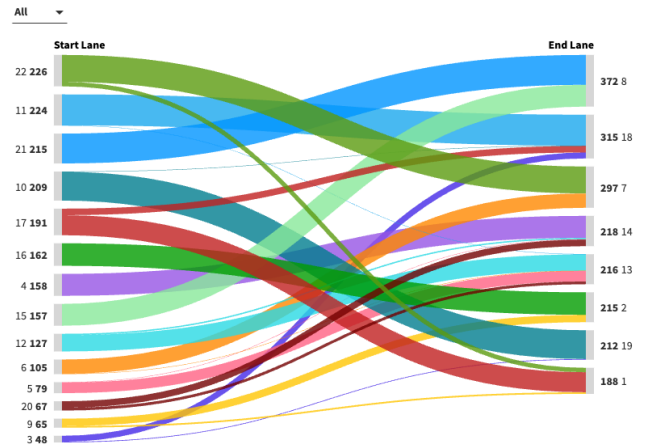


Fig. 4. Transition from start lane to end lane in scenario WGM_N

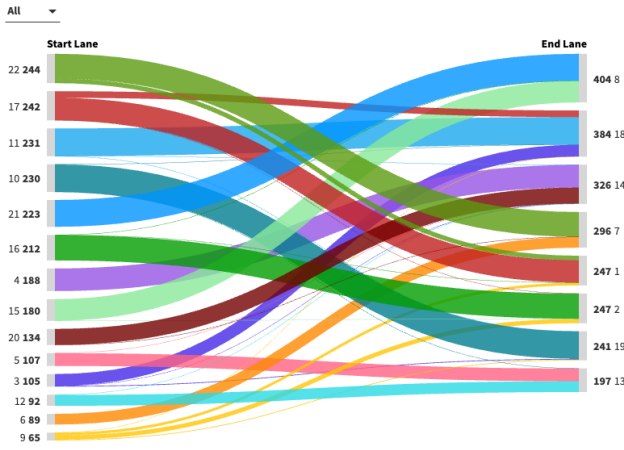


Fig. 5. Transition from start lane to end lane in scenario WGM_AN

3) *Traffic Density Analysis*: Figure 6 presents the traffic density per minute over 60 minutes at four intersections, offering a more granular view of traffic patterns throughout the observation periods. In GWG intersection, at noon density ranges between 25 to 35 while the range increases which is 35 to 45 in the afternoon. In WGM intersection, at noon, the density is high and stable compared to the afternoon data. At noon, density ranges from 35 to 45 while in the afternoon, density ranges from 35 to 42 with a high amount of fluctuation.

The erratic afternoon patterns at WGM intersection likely result from multiple factors interacting during the blackout. Without traffic signals, drivers must navigate the intersection independently, causing uneven traffic density. This effect is more pronounced during busy afternoons, which creates alternating periods of congestion and rapid clearance. Driver adaptation to unusual conditions, varying levels of caution and assertiveness, and the diverse mix of trip purposes typical of afternoon traffic could further contribute to the inconsistent flow.

4) *Comparison with Benchmark Dataset*: We compare the proposed Beacon dataset with previous datasets that were collected at intersections in urban areas. Table II listed three traffic datasets, their size, collected method, and weather/environment/specialty of the scenes. Other intersection datasets were collected from urban intersections and easily availability of urban intersections and having huge amounts of daily traffic density in the intersections the size of these datasets is much larger than Beacon. However, we can see Beacon is the only dataset that has been collected from urban intersections during traffic light blackouts. Besides, Beacon has used the least amount of instruments to collect the dataset, which eventually results in the most cost-effective data.

TABLE II
COMPARISON WITH OTHER INTERSECTION DATASETS

Dataset	Size	Scene	Collection Method	Weather
INTERACTION [20]	110K trajectories	(un)signalized intersection	UAV, V2X	–
USyd [21]	24K trajectories	5 intersections	onboard	–
V2X-Seq [22]	50K scenarios	28 urban intersections	V2X	–
Beacon	8811 vehicles	(un)signalized intersections	single camera	TL Blackout

IV. RECONSTRUCTION OF UNSIGNALIZED INTERSECTIONS

A. Data Transformation and Network Validation

We utilize OpenStreetMap (OSM) [23] to select the specific area in Memphis, TN, USA that encompasses the the Walnut Grove-Goodlett and Walnut Grove-Mendenhall intersections. For traffic simulation, we employ SUMO (Simulation of Urban Mobility) [24]. We utilize SUMO's NETCONVERT tool to transform the extracted OSM data into a .net.xml file, which is the standard network file format used by SUMO. During this conversion process, we pay particular attention to preserving the integrity and accuracy of road characteristics from the original OSM data. This includes ensuring correct lane numbers, intersection layouts, and road geometries. The resulting .net.xml file provides a detailed digital representation of the road network, serving as the basis for our traffic simulations.

We assigned integer numbers to lanes for each scenario for labeling convenience, as shown in Fig. 1. However, SUMO automatically assigns unique IDs to lanes in its network file. During data processing, we mapped our integer IDs to SUMO's IDs to accurately reconstruct traffic patterns. Fig. 1 shows the renditions of the two intersections in SUMO. We get each vehicle's timestep when it is in the head of the start lane and start lane and end lane information from the Beacon dataset using TRACI and then add vehicles to the simulation. As the start lane and end lane of each vehicle together give us the route for that vehicle we imported the route information for each vehicle in the SUMO route files.

B. Correctness of the Reconstruction

To evaluate the accuracy of our traffic reconstruction, we compare the simulated traffic patterns with the observed data. Table III presents the results of this comparison across all four scenarios.

We focus on three types of potential mismatches. Table III listed no mismatches of the start lane meaning all vehicles started from the lane that was supposed to start. Though vehicles' timestep information was imported simultaneously to the simulation from the beacon dataset sometimes SUMO delayed generating some vehicles to the simulation. After crossing the intersections, some vehicles chose lanes different

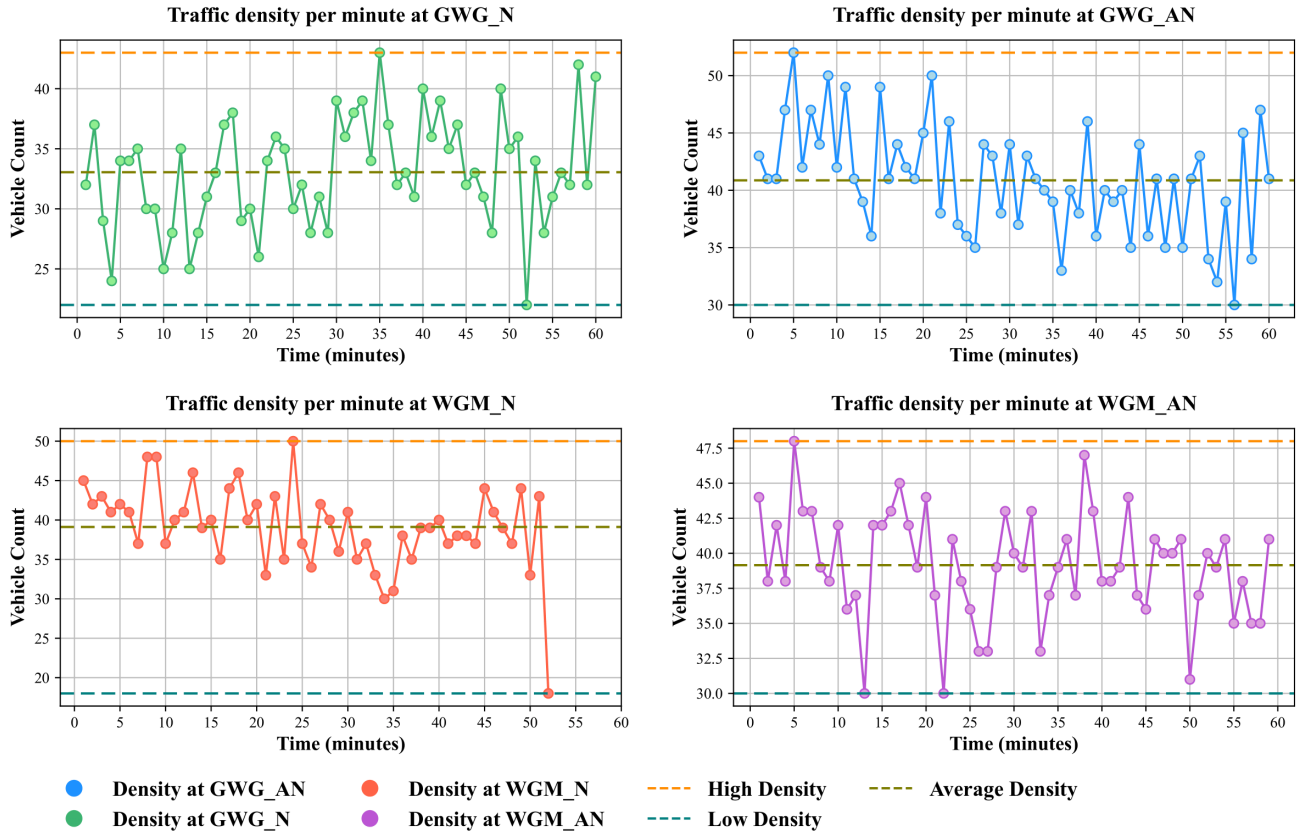


Fig. 6. Traffic density per minute at four intersection scenes

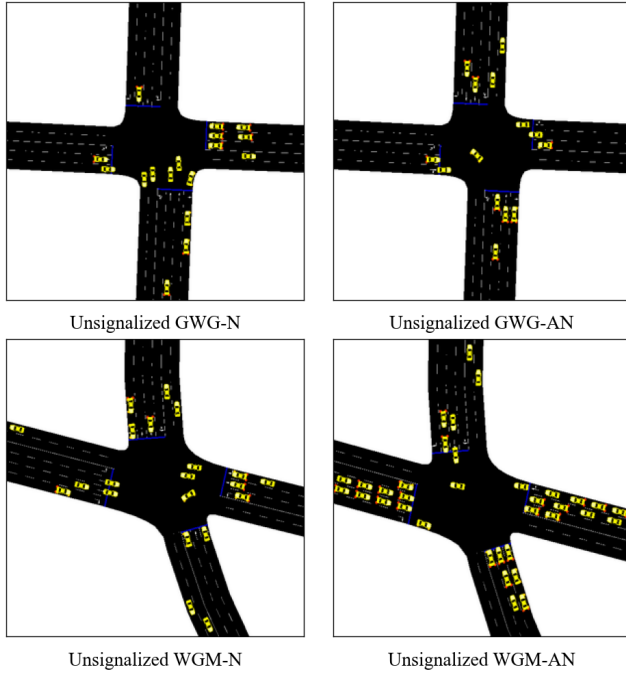


Fig. 7. Unsignalized reconstruction of Beacon dataset for intersection GWG-N (upper-left), GWG-AN (upper-right), WGM-N (lower-left), WGM-AN (lower-right) in SUMO

TABLE III
CORRECTNESS OF THE RECONSTRUCTION OF UNSIGNALIZED TRAFFIC SCENARIOS FROM DATASET

Scenario	Number of cars	timestep mismatch	Start mismatch	End mismatch	Total mismatch	%
GWG-AN	2452	10	0	0	10	0.41
GWG-N	1962	38	0	0	38	1.93
WGM-N	2032	5	0	191	196	8.4
WGM-AN	2342	6	0	199	205	8.75

from the dataset's end lane. We suspect that these vehicles follow the free flow available in other lanes. Thus, a few timestep and end lane mismatches happened which was beyond our control.

- Timestep mismatch: Differences in the timing of vehicle movements between the observed and simulated data.
- Start mismatch: Discrepancies in the starting lanes of vehicles entering the intersection.
- End mismatch: Differences in the exit lanes of vehicles leaving the intersection.

Results show high accuracy for the Walnut Grove-Goodlett intersection, with mismatch rates of 0.41% and 1.93% for evening and midday scenarios, respectively. The Walnut Grove-Mendenhall intersection exhibit higher mismatch rates (8.4% and 8.75%), primarily due to end mismatches, suggesting challenges in simulating more complex intersections

under blackout conditions.

V. RECONSTRUCTION OF SIGNALIZED INTERSECTIONS

Building upon our earlier work in extracting the road network from OpenStreetMap in section IV, we also reconstruct the four scenarios with traffic lights.

A. Traffic Light Phase Implementation

For Walnut Grove-Goodlett intersection, we implement a fixed traffic phase timing for all four directions. The phase for each direction over time is shown in Figure 9 (left). The phase sequence repeats as 7, 4, 29, 4, 20, 4, 4, 40, and 4 seconds. Each phase allocates green, yellow, and red lights to specific directions, ensuring orderly traffic flow.

For Walnut Grove-Mendenhall intersection, we use a different phase timing sequence: 22, 4, 80, 4, 42, 4, 4, 113, and 4 seconds, illustrated in Figure 9 (right). This sequence follows a similar pattern of allocating green, yellow, and red lights to various directions, but with longer duration to accommodate different traffic patterns at this intersection.

B. Correctness of the Reconstruction

To validate our reconstruction, we compare simulated and observed data, as shown in Table IV. Since it is signalized reconstruction and vehicles may need to wait to cross the intersection, the timesteps may not match in simulation with Beacon dataset. Results showed high accuracy for the Walnut Grove-Goodlett intersection (0.612% and 4.49% mismatch rates for midday and afternoon scenarios). The Walnut Grove-Mendenhall intersection had higher mismatch rates (14.13% and 15.77%), indicating challenges in simulating complex intersections under signalized conditions.

TABLE IV

CORRECTNESS OF THE RECONSTRUCTION OF SIGNALIZED TRAFFIC SCENARIOS FROM DATASET

Scenario	Number of cars	Start mismatch	End mismatch	Total	%
GWG-N	1961	0	12	12	0.612
GWG-AN	2135	0	96	96	4.49
WGM-N	2031	0	287	287	14.13
WGM-AN	2340	0	369	369	15.77

VI. RECONSTRUCTION OF MIXED TRAFFIC IN INTERSECTIONS

Mixed traffic control, where robot vehicles (RV) control surrounding robot vehicles and human-driven vehicles (HV) to accomplish some task (i.e. alleviate congestion), under unsignalized intersections has seen recent research [25]. In particular, RVs can coordinate traffic at complex intersections without traditional traffic signals, achieving significant improvement in traffic efficiency and even eco-driving [26]–[33].

Fig. 10 shows Beacon reconstructed under mixed traffic for Traffic Scenario 3 and Traffic Scenario 4 where red vehicles are RVs and white vehicles are HVs. Each scenario has 50%

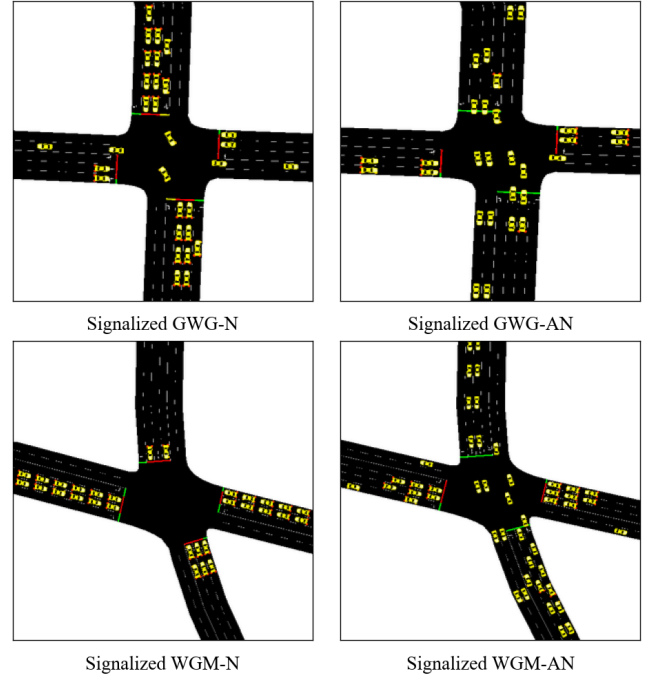


Fig. 8. Signalized reconstruction of Beacon dataset for intersection GWG-N (upper-left), GWG-AN (upper-right), WGM-N (lower-left), WGM-AN (lower-right) in SUMO

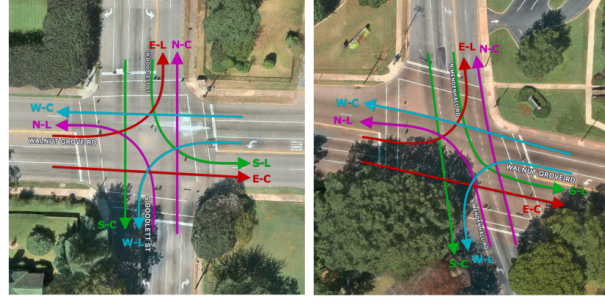
RV penetration rate, but any penetration rate in the range [0, 100] can be selected.

The results in Table V reveal that the effectiveness of RVs is highly dependent on the traffic volume. At the simpler Walnut Grove-Goodlett intersection, RVs show limited benefits under normal traffic condition, suggesting that traffic volumes haven't reached a threshold where RV coordination significantly outperforms human drivers. Conversely, at the more complex Walnut Grove-Mendenhall intersection, RVs demonstrate substantial improvements in wait times and travel times, particularly during high-traffic periods.

To further investigate the traffic volume threshold hypothesis, we conduct additional simulations at the Walnut Grove-Goodlett intersection, increasing the traffic demand at each direction from Scenario 1 by 25% and 50%. Table VI presents the results. With a 25% increase in demand, we observe that incorporating RVs reduces wait times by up to 82.6% and travel time by 10.3%. However, this improvement comes with a 7.2% increase in CO2 emissions. The benefits of RVs become even more pronounced with a 50% increase in traffic demand. RVs decrease the overall wait times by 47.1%, and travel times by 21.8%. As wait times decrease and throughput increases with higher RV penetration, we observe a corresponding increase in CO2 emissions. This is consistent with vehicles spending less time idling and more time moving at higher speeds, which typically results in higher emission rates.

VII. CONCLUSION

The Beacon study provides insights into urban traffic dynamics during blackouts through the analysis of naturalistic



Traffic Light Phases for GWG intersection

Traffic Light Phases for WGM intersection

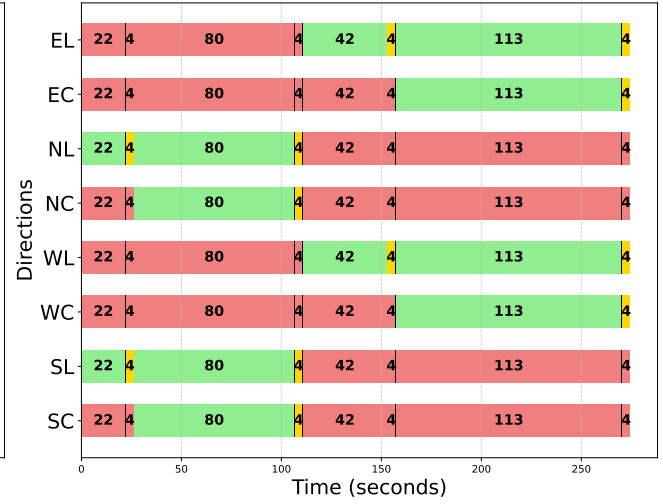
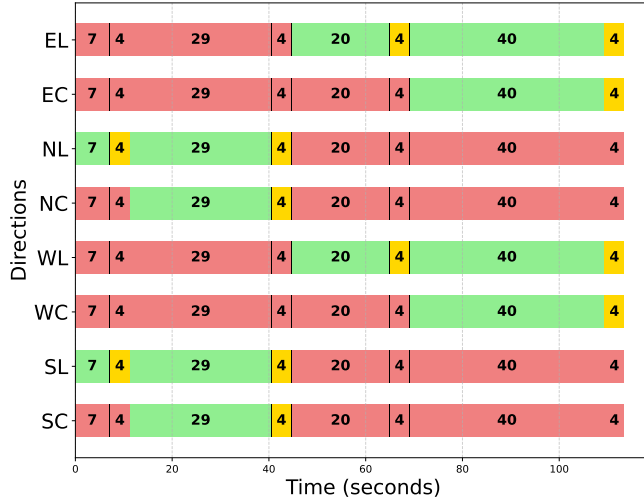


Fig. 9. Traffic light phases for GWG and WGM intersection

driving data from two intersections in Memphis, TN. Our findings demonstrate the potential benefits of integrating robot vehicles for traffic management under these conditions, particularly in high-volume conditions. The reconstruction of various traffic conditions - unsignalized, signalized, and mixed - showcases the utility of Beacon while also revealing areas for improvement in modeling approaches. Future work will focus on improving traffic simulation accuracy and expanding the dataset for broader application, enhancing urban traffic resilience.

There are many future directions to pursue. First, we would like to integrate the insights of this project with existing techniques [34]–[38] to further enable the learning, planning, and robustness of robot vehicles. Second, we want to extend our study to large-scale traffic simulation, reconstruction, and prediction [39]–[48] to benefit various intelligent transportation systems applications. Lastly, we want to test our network optimization algorithm [49] on various levels of reconstruction tasks.

REFERENCES

- [1] A. Press, “Power still out to 50k customers, days after memphis storm,” <https://www.usnews.com/news/best-states/tennessee/articles/2022-02-07/power-still-out-to-60k-customers-days-after-memphis-storm>, Feb. 2022.
- [2] E.-H. Choi, “Crash factors in intersection-related crashes: An on-scene perspective,” *National Highway Traffic Safety Administration, U.S. Department of Transportation*, 2010.
- [3] B. Winck, “Get ready for blackouts from london to la, as the global energy crisis overwhelms grids and sends energy prices skyrocketing,” <https://www.businessinsider.com/global-europe-energy-crisis-power-electricity-outages-blackouts-energy-grid-2022-9>, Sept. 2022.
- [4] R. Ramirez, “Power outages are on the rise, led by texas, michigan and california. here’s what’s to blame,” <https://www.cnn.com/2022/09/14/us/power-outages-rising-extreme-weather-climate/index.html>, Sept. 2022.
- [5] E. R. Sanchez, S. Raghavan, and C. Wu, “Data-driven traffic reconstruction and kernel methods for identifying stop-and-go congestion,” *arXiv preprint arXiv:2312.03186*, 2023.
- [6] Y. Wang, Y. Zhang, X. Piao, H. Liu, and K. Zhang, “Traffic data reconstruction via adaptive spatial-temporal correlations,” *IEEE Transactions on Intelligent Transportation Systems*, vol. 20, no. 4, pp. 1531–1543, 2018.
- [7] S. Kataoka, M. Yasuda, C. Furtlehner, and K. Tanaka, “Traffic data reconstruction based on markov random field modeling,” *Inverse Problems*, vol. 30, no. 2, p. 025003, 2014.
- [8] S. Bilotta and P. Nesi, “Traffic flow reconstruction by solving indeterminacy on traffic distribution at junctions,” *Future Generation Computer Systems*, vol. 114, pp. 649–660, 2021.
- [9] X. Qi, Y. Ji, W. Li, and S. Zhang, “Vehicle trajectory reconstruction on urban traffic network using automatic license plate recognition data,” *IEEE Access*, vol. 9, pp. 49 110–49 120, 2021.
- [10] Y. Feng, J. Sun, and P. Chen, “Vehicle trajectory reconstruction using automatic vehicle identification and traffic count data,” *Journal of advanced transportation*, vol. 49, no. 2, pp. 174–194, 2015.
- [11] P. Bellini, S. Bilotta, P. Nesi, M. Paolucci, and M. Soderi, “Wip: traffic flow reconstruction from scattered data,” in *2018 IEEE International*

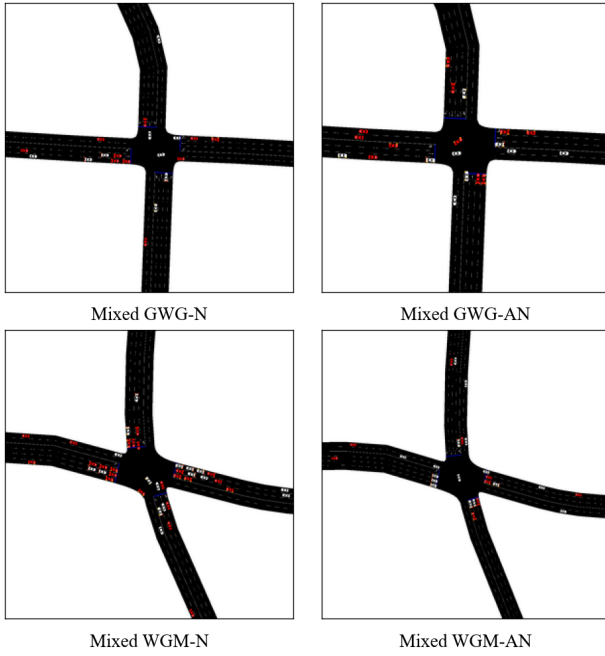


Fig. 10. The figure shows all four scenarios using Beacon: (a) GWG-N(upper-left), (b)GWG-AN(upper-right), (c) WGM-N(lower-left), and (d) WGM-AN(lower-right) reconstructed with mixed traffic. The red vehicles are robot vehicles (RV), and the white vehicles are human-driven vehicles (HV). The RV penetration rate is 50%; however, the penetration rate can be adjusted to any percent in the range [0, 100]. Reconstructing Beacon under mixed traffic scenarios allows for mixed traffic control where RVs learn to take intelligent actions to improve traffic flow in the scenarios.

Conference on Smart Computing (SMARTCOMP). IEEE, 2018, pp. 264–266.

- [12] A. Bakowski and L. Radziszewski, “Measurements of urban traffic parameters before and after road reconstruction,” *Open Engineering*, vol. 11, no. 1, pp. 365–376, 2021.
- [13] M. Čičić, M. Barreau, and K. H. Johansson, “Numerical investigation of traffic state reconstruction and control using connected automated vehicles,” in *2020 IEEE 23rd International Conference on Intelligent Transportation Systems (ITSC)*. IEEE, 2020, pp. 1–6.
- [14] Z. Shen, W. Ji, S. Yu, G. Cheng, Q. Yuan, Z. Han, H. Liu, and T. Yang, “Mapping the knowledge of traffic collision reconstruction: A scientometric analysis in citespace, vosviewer, and scimat,” *Science & Justice*, vol. 63, no. 1, pp. 19–37, 2023.
- [15] Q. Li, Z. M. Peng, L. Feng, Z. Liu, C. Duan, W. Mo, and B. Zhou, “Scenarionet: Open-source platform for large-scale traffic scenario simulation and modeling,” *Advances in neural information processing systems*, vol. 36, 2024.
- [16] P. Sun, H. Kretschmar, X. Dotiwalla, A. Chouard, V. Patnaik, P. Tsui, J. Guo, Y. Zhou, Y. Chai, B. Caine, *et al.*, “Scalability in perception for autonomous driving: Waymo open dataset,” in *Proceedings of the IEEE/CVF conference on computer vision and pattern recognition*, 2020, pp. 2446–2454.
- [17] H. Caesar, V. Bankiti, A. H. Lang, S. Vora, V. E. Liong, Q. Xu, A. Krishnan, Y. Pan, G. Baldan, and O. Beijbom, “nuscenes: A multimodal dataset for autonomous driving,” in *Proceedings of the IEEE/CVF conference on computer vision and pattern recognition*, 2020, pp. 11 621–11 631.
- [18] M.-F. Chang, J. Lambert, P. Sangkloy, J. Singh, S. Bak, A. Hartnett, D. Wang, P. Carr, S. Lucey, D. Ramanan, *et al.*, “Argoverse: 3d tracking and forecasting with rich maps,” in *Proceedings of the IEEE/CVF conference on computer vision and pattern recognition*, 2019, pp. 8748–8757.
- [19] Q. Li, Z. Peng, L. Feng, Q. Zhang, Z. Xue, and B. Zhou, “Metadrive: Composing diverse driving scenarios for generalizable reinforcement learning,” *IEEE Transactions on Pattern Analysis and Machine Intelligence*, 2022.
- [20] Z. Wei, “Interaction dataset: an international, adversarial and coop-

TABLE V
PERFORMANCE METRICS FOR MIXED TRAFFIC SCENARIOS WITH VARYING RV PENETRATION RATES ACROSS FOUR INTERSECTION SCENARIOS

Scenario	Metric	HVs	RV Penetration Rate				
			20%	40%	60%	80%	100%
GWG-N	Wait Time (s)	0.16	0.19	0.27	0.44	0.47	0.41
	Travel Time (s)	83.82	84.38	84.79	86.08	86.25	86.22
	CO ₂ Emissions (mg/s)	1642	1644	1640	1627	1626	1630
GWG-AN	Wait Time (s)	0.78	3.20	2.73	2.86	3.56	2.59
	Travel Time (s)	65.01	68.34	65.80	67.47	68.04	64.61
	CO ₂ Emissions (mg/s)	3842	3405	3501	3424	3350	3529
WGM-N	Wait Time (s)	3.60	3.72	3.08	2.56	1.52	1.88
	Travel Time (s)	112.06	112.43	109.39	104.90	99.72	103.62
	CO ₂ Emissions (mg/s)	1452	1402	1422	1443	1493	1470
WGM-AN	Wait Time (s)	16.21	2.11	1.71	1.98	1.72	1.06
	Travel Time (s)	127.36	98.86	98.16	100.44	99.00	95.73
	CO ₂ Emissions (mg/s)	1323	1535	1537	1514	1527	1550

TABLE VI
PERFORMANCE METRICS FOR WALNUT GROVE-GOODLETT INTERSECTION WITH INCREASED TRAFFIC DEMAND

Demand Increase	Metric	HVs	RV Penetration Rate				
			20%	40%	60%	80%	100%
25%	Wait Time (s)	6.48	7.81	4.15	2.33	1.13	3.06
	Travel Time (s)	95.53	97.14	91.48	88.44	85.72	90.47
	CO ₂ Emissions (mg/s)	1703	1707	1759	1793	1825	1799
50%	Wait Time (s)	63.19	49.18	43.33	36.60	33.47	52.31
	Travel Time (s)	166.97	162.92	146.27	136.06	130.51	129.39
	CO ₂ Emissions (mg/s)	1440	1489	1522	1565	1596	1864

erative motion dataset in interactive driving scenarios with semantic maps,” *arXiv: 1910.03088*, 2019.

- [21] A. Zyner, S. Worrall, and E. Nebot, “Naturalistic driver intention and path prediction using recurrent neural networks,” *IEEE transactions on intelligent transportation systems*, vol. 21, no. 4, pp. 1584–1594, 2019.
- [22] H. Yu, W. Yang, H. Ruan, Z. Yang, Y. Tang, X. Gao, X. Hao, Y. Shi, Y. Pan, N. Sun, *et al.*, “V2x-seq: A large-scale sequential dataset for vehicle-infrastructure cooperative perception and forecasting,” in *Proceedings of the IEEE/CVF Conference on Computer Vision and Pattern Recognition*, 2023, pp. 5486–5495.
- [23] OpenStreetMap contributors, “Openstreetmap,” <https://www.openstreetmap.org>, 2013, accessed: 2023-03-25.
- [24] P. A. Lopez, M. Behrisch, L. Bieker-Walz, J. Erdmann, Y.-P. Flötteröd, R. Hilbrich, L. Lücken, J. Rummel, P. Wagner, and E. Wießner, “Microscopic traffic simulation using sumo,” in *The 21st IEEE International Conference on Intelligent Transportation Systems*. IEEE, 2018. [Online]. Available: <https://elib.dlr.de/124092/>
- [25] A. Gholamhosseinian and J. Seitz, “A comprehensive survey on cooperative intersection management for heterogeneous connected vehicles,” *IEEE Access*, vol. 10, pp. 7937–7972, 2022.
- [26] I. Islam, W. Li, S. Li, and K. Heaslip, “Heterogeneous mixed traffic control and coordination,” in *Heterogeneous Mixed Traffic Control and Coordination*, 2024.
- [27] D. Wang, W. Li, L. Zhu, and J. Pan, “Learning to control and coordinate mixed traffic through robot vehicles at complex and unsignalized intersections,” *International Journal of Robotics Research*, 2024.
- [28] D. Wang, W. Li, and J. Pan, “Large-scale mixed traffic control using

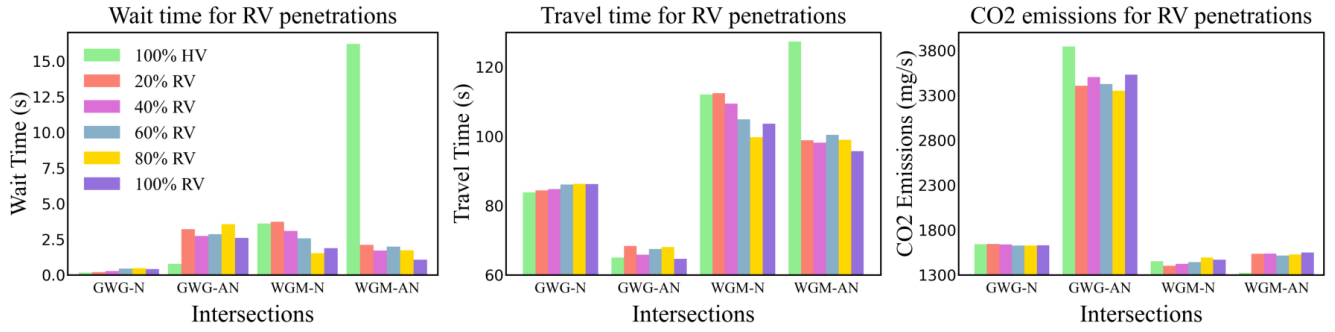


Fig. 11. Comparison of wait time (left), travel time (center) and CO2 emission (right) for varying RV penetration rates in controlled mixed traffic scenarios at four intersections

- dynamic vehicle routing and privacy-preserving crowdsourcing,” *IEEE Internet of Things Journal*, vol. 11, no. 2, pp. 1981–1989, 2024.
- [29] B. Poudel, W. Li, and S. Li, “Carl: Congestion-aware reinforcement learning for imitation-based perturbations in mixed traffic control,” in *International Conference on CYBER Technology in Automation, Control, and Intelligent Systems (CYBER)*, 2024.
- [30] B. Poudel, W. Li, and K. Heaslip, “Endurl: Enhancing safety, stability, and efficiency of mixed traffic under real-world perturbations via reinforcement learning,” in *IEEE/RSJ International Conference on Intelligent Robots and Systems (IROS)*, 2024.
- [31] M. Villarreal, D. Wang, J. Pan, and W. Li, “Analyzing emissions and energy efficiency in mixed traffic control at unsignalized intersections,” in *IEEE Forum for Innovative Sustainable Transportation Systems (FISTS)*, 2024, pp. 1–7.
- [32] M. Villarreal, B. Poudel, J. Pan, and W. Li, “Mixed traffic control and coordination from pixels,” in *IEEE International Conference on Robotics and Automation (ICRA)*, 2024, pp. 4488–4494.
- [33] M. Villarreal, B. Poudel, and W. Li, “Can chatgpt enable its? the case of mixed traffic control via reinforcement learning,” in *IEEE International Conference on Intelligent Transportation Systems (ITSC)*, 2023, pp. 3749–3755.
- [34] W. Li, D. Wolinski, and M. C. Lin, “ADAPS: Autonomous driving via principled simulations,” in *IEEE International Conference on Robotics and Automation (ICRA)*, 2019, pp. 7625–7631.
- [35] Y. Shen, W. Li, and M. C. Lin, “Inverse reinforcement learning with hybrid-weight trust-region optimization and curriculum learning for autonomous maneuvering,” in *IEEE/RSJ International Conference on Intelligent Robots and Systems (IROS)*, 2022, pp. 7421–7428.
- [36] L. Lin, W. Li, H. Bi, and L. Qin, “Vehicle trajectory prediction using LSTMs with spatial-temporal attention mechanisms,” *IEEE Intelligent Transportation Systems Magazine*, vol. 14, no. 2, pp. 197–208, 2022.
- [37] Y. Shen, L. Zheng, M. Shu, W. Li, T. Goldstein, and M. C. Lin, “Gradient-free adversarial training against image corruption for learning-based steering,” in *Advances in Neural Information Processing Systems (NeurIPS)*, 2021, pp. 26 250–26 263.
- [38] M. Villarreal, B. Poudel, R. Wickman, Y. Shen, and W. Li, “Autojoin: Efficient adversarial training for robust maneuvering via denoising autoencoder and joint learning,” in *IEEE/RSJ International Conference on Intelligent Robots and Systems (IROS)*, 2024.
- [39] D. Wilkie, J. Sewall, W. Li, and M. C. Lin, “Virtualized traffic at metropolitan scales,” *Frontiers in Robotics and AI*, vol. 2, p. 11, 2015.
- [40] W. Li, D. Wolinski, and M. C. Lin, “City-scale traffic animation using statistical learning and metamodel-based optimization,” *ACM Trans. Graph.*, vol. 36, no. 6, pp. 200:1–200:12, 2017.
- [41] W. Li, D. Nie, D. Wilkie, and M. C. Lin, “Citywide estimation of traffic dynamics via sparse GPS traces,” *IEEE Intelligent Transportation Systems Magazine*, vol. 9, no. 3, pp. 100–113, 2017.
- [42] W. Li, M. Jiang, Y. Chen, and M. C. Lin, “Estimating urban traffic states using iterative refinement and wardrop equilibria,” *IET Intelligent Transport Systems*, vol. 12, no. 8, pp. 875–883, 2018.
- [43] L. Lin, W. Li, and S. Peeta, “Efficient data collection and accurate travel time estimation in a connected vehicle environment via real-time compressive sensing,” *Journal of Big Data Analytics in Transportation*, vol. 1, no. 2, pp. 95–107, 2019.
- [44] —, “Predicting station-level bike-sharing demands using graph convolutional neural network,” in *Transportation Research Board 98th Annual Meeting (TRB)*, 2019.
- [45] Q. Chao, H. Bi, W. Li, T. Mao, Z. Wang, M. C. Lin, and Z. Deng, “A survey on visual traffic simulation: Models, evaluations, and applications in autonomous driving,” *Computer Graphics Forum*, vol. 39, no. 1, pp. 287–308, 2020.
- [46] B. Poudel and W. Li, “Black-box adversarial attacks on network-wide multi-step traffic state prediction models,” in *IEEE International Conference on Intelligent Transportation Systems (ITSC)*, 2021, pp. 3652–3658.
- [47] L. Lin, W. Li, and L. Zhu, “Data-driven graph filter based graph convolutional neural network approach for network-level multi-step traffic prediction,” *Sustainability*, vol. 14, no. 24, p. 16701, 2022.
- [48] K. Guo, Z. Miao, W. Jing, W. Liu, W. Li, D. Hao, and J. Pan, “Lasil: Learner-aware supervised imitation learning for long-term microscopic traffic simulation,” in *IEEE/CVF Conference on Computer Vision and Pattern Recognition (CVPR)*, 2024, pp. 15 386–15 395.
- [49] R. Wickman, X. Zhang, and W. Li, “A generic graph sparsification framework using deep reinforcement learning,” in *IEEE International Conference on Data Mining (ICDM)*, 2022, pp. 1221–1226.